TOWARDS A COMPREHENSIVE COLOR STEREOSCOPIC MATCHING MODEL BASED ON HVS BEHAVIOR

Rafik BENSALMA, Mohamed-Chaker LARABI

XLIM lab., SIC dept., University of Poitiers
Poitiers, France
Email: bensalma,larabi@sic.univ-poitiers.fr

ABSTRACT

3D applications need a stereo matching algorithm that can merge the left image with the right image. In this paper we propose a stereo matching algorithm based on some binocular properties of the human visual system. For this, we have focused on the simple and complex cells properties that are responsible for binocular fusion. A model, based on a complex wavelet transform, a color contrast sensitivity function and a bandelet transform, is proposed to model the properties of the simple and complex cells characterized by their size, orientation, phase and amplitude. This model is designed to calculate the binocular energy generated by each binocular complex cell. A model refinement based on properties specific to the lateral geniculate body is then proposed to refine the results obtained with the binocular energy model calculation. The obtained results can be exploited by the stereoscopic vision applications, such as 3D reconstruction, stereoscopic coding, stereoscopic quality assessment and other applications.

1. INTRODUCTION

The binocular vision has the responsibility to put both eyes in a synchronous way and with a perfect coordination to reconstruct the relief. The retinal images received by both eyes go through a succession of processes before arriving to the visual cortex where they are merged. More and more work has been done to model the match operation which both images undergo at the visual cortex. Hubel and wisel [1] defined two types of binocular cells, named as the simple and the complex cells, according to the degree of their complexity. The complex cells, in their model, are built by association of a set of simple cells as described by Fig. 1. According to Hubel et al. [1] and campbell et al.[2] the receiving fields of these cells are described as a linear filter constituted by different activated regions (ON) and inhibited regions (OFF). The optimal activation of these cells is made by a luminance grating so that the white bar covers the ON region and the black bar covers the OFF region. In 1990, Ohzawa et al.[3] proposed a model to compute the binocular energy. They model the cells by functions characterized by their amplitude and orientation. In literature, orientation selective wavelets as the Gabor wavelet, the curvelet and the bandelet describe mathematically the functioning of these cells. The ON and OFF regions of the cells correspond respectively to peaks and hollows of these functions.

In this paper, we propose a matching algorithm taking into account the phenomenon of binocular rivalry. The paper is organized in four sections: In the second section, we present the proposed approach; Our model for computing the binocular energy is introduced in the third section, the fourth section focuses on the refinement of the model; The experimental results are presented in section five. This paper ends with some conclusions and gives some future directions.

2. PROPOSED FTOAPPROACH

The binocular matching is the most complex process in the stereoscopic vision. To conceive our model we are interested in the functioning of the human visual system (HVS). Once the retinal images are captured by both retinas, the left halves of the images are stored in the right lateral geniculate body (LGB) and the right halves are stored in the left LGB. Two signals belonging to the right and left retinal images and representing the same region of the space are put side by side.

The binocular rivalry phenomenon appears when both retinal images are different; The LBG replaces the stimulus having the least contrast by the stimulus with the highest contrast. To simulate these processes, in the aim to optimize the matching, we integrated binocular constraints and monocular constraints in our model. The binocular constraints used in our model are the uniqueness constraint, occlusion constraint and the cohesiveness constraint. The monocular constraints used are occlusion, cohesiveness and inter-ocular inhibition constraints described in Section. 4. The last constraint allows to take into account the binocular rivalry phenomenon in our model.

After these pretreatments, the signals leave the LGB for the visual cortex. In the visual cortex, we have the simple and the complex cells, which are responsible for the binocular fusion. These cells are characterized by their size, phase and orientation. The signals from the two LGBs are classified into two categories, the monocular signals captured by the monocular simple cells and the binocular signals captured by binocular simple cells. The simple cells work in pairs (Fig. 1); each pair is connected to a complex cell. The simple cells of one pair have the same size and orientation with a phase shift equal to $\pi/2$. The first cell has a center sensitive to light and a circumference not sensitive to light (ON/OFF) and the opposite is true for the other cell, a center not sensitive to light and a circumference sensitive to light (OFF/ON). For that reason there is a phase shift between the cells pair.

To model the behavior of these cells, we looked at the adaptive spatial frequency transform presenting the same mathematical properties with these cells. In the first step, we applied the complex wavelet transform (CWT) on both stereoscopic images. The analysis functions used to obtain the real and imaginary part of this decomposition has a phase shift equal to $\pi/2$. This decomposition allows to separate the response obtained with both types of simple cells (ON/OFF) and (OFF/ON). After this stage, a contrast sensitivity func-

 ISSN 2076-1465

tion (CSF) [4] is applied on the coefficients obtained with the complex wavelet transform. This function allows to remove the CWT coefficients that are not perceived by the human visual system, which gives a better representation of the singularities of stereoscopic images in the complex wavelets domain. To identify the pairs of simple cells, we applied the bandelet transform on the coefficients obtained with the CWT. The same geometry (quad-tree, orientation) is used in the bandelet transform for real and imaginary parts of the CWT. The good representation of the singularities, of the two stereoscopic images obtained with CSF, allows a better estimation of the geometry of the images obtained by bandelet transform.

Two dyadic squares, which belong respectively to real and imaginary parts of the left or the right image, constitute a pair of response having the same characteristics (size, orientation and phase) with simple pair of cells. These pairs of dyadic squares areare exploited by a model for computing a binocular energy of the retinal images.

3. BINOCULAR ENERGY MODEL (BEM)

In the previous section, we mentioned the spatial-frequency transform that we use in our metric scheme. As shown in the following figure, a CWT is applied to the luminance component $[L^*]$ of the left and right retinal images. The filters used to compute the real and the imaginary parts presents a shift-phase equal to $\pi/2$. DWT is applied to the chromatic component of the both images (a^* and b^*), knowing that these components are orthogonal. This preprocessing step allows a complex writing of the luminance and chrominance components as described by equation 1.

$$\begin{aligned} Image &= \{Re[L], Im[L], Re[C], Im[C]\} \\ &= \{Re[CWT(L^*)], Im[CWT(L^*)], DWT[C(a^*)], DWT[C(b^*)]\} \\ &L: luminance, C: Chrominance \end{aligned} \quad (1)$$

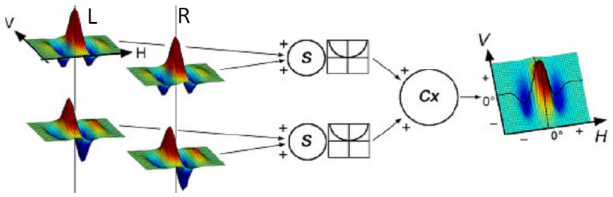

Fig. 1. Simplistic representation of the dyadic squares to be matched.

Starting from the definition given above, the model that we propose to calculate the binocular energy is based on the model proposed by Ohzawa [3] and the one proposed by Fleet [5]. Bandelet transform, applied on the wavelet coefficients of luminance and chrominance components, allows to define the image geometry. This latter is defined by a set of dyadic squares (the same geometry is applied to the real and imaginary parts of the luminance and chrominance). Each dyadic square is characterized by its size and orientation. Dyadic squares obtained with CWT applied to the luminance are arranged in pairs, similar to the dyadic squares obtained with the DWT, applied to both chrominance components. Dyadic squares of a given pair belong to the real part of the CWT ($Re[L(x)]^L$) and the imaginary part of the CWT ($Im[L(x)]^L$). Dyadic square pairs of the chromatic component belong respectively to the real part represented by the DWT ($Re[L(x)]^C$), applied to the component a^* and the imaginary part represented by the DWT ($Im[L(x)]^C$), applied to the component b^*. Dyadic squares of a pair have given the same orientation and same size with a shift-phase equal to $\pi/2$. $L(x)$ and $R(x)$ (responses of two simple cells (Fig. 1)), Complex-valued response in left and right eyes, are expressed by their amplitude and orientation of the complex function($L(x) = \rho_l(x)\exp(\phi_l(x))$). where:

$$\rho_l^2(x) = |L(x)|^2 = Re[L(x)]^2 + Im[L(x)]^2 \quad (2)$$

$\rho_l(x)$ is the monocular amplitude of the complex function and $\phi_l(x)$(Eq. 3) is the phase monocular of the complex function.

$$\phi_l(x) = arg|L(x)| = arctan(Im[L(x)]/RE[L(x)]) \quad (3)$$

Table 1 summarizes all the parameters described above by giving the appropriate definition.

Table 1. Symbol table.

parameters	Definitions
X	Retinal position
L(x), R(x)	Complex-valued response in left and right eyes, at position x
$Re[L(x)]^L$	Luminance real part of left monocular response(dyadic square)
$Im[L(x)]^L$	Luminance imaginary part of left monocular response
$Re[L(x)]^C$	Color real part of left monocular response
$Im[L(x)]^C$	Color imaginary part of left monocular response
$\rho_{l/r}(x)$	Monocular (left eye) amplitude signal
$\phi_{l/r}(x)$	Monocular (left eye) phase signal
$\phi'_{l/r}(x)$	Left-eye instantaneous frequency at position x
$\Delta\psi$	simple cell phase shift
d	Stimulus disparity
$\Delta\phi(x)$	phase difference
$E(x)$	Binocular energy response at retinal position x
$E(x,d)$	Response of binocular energy neuron with simple cell position shift
$E(x,\Delta\psi)$	Response of binocular energy neuron with simple cell phase shift
$E(x,d,\Delta\psi)$	Response of binocular hybrid energy neuron with position shift d and phase shift $\Delta\psi$

After all the preprocessing steps comes the stage of matching of the retinal pairs of images. For this, the dyadic squares pair of one image are matched with another pair of the second image by calculating the binocular energy produced by these two pairs of dyadic squares (which represents the response of two simple cells). The cell responsible of the information fusion, in the human visual system, is the complex cell. The binocular complex cell takes as input two responses from two simple cells (two pairs of dyadic squares belonging respectively to the left and right retinal images). If the complex cell is of type monocular, it will take as input a response of a simple cell (a pair of dyadic squares). In the case of a binocular complex cell, the binocular energy (Eq. 11) is calculated as described in [5].

$$\begin{aligned} E(x) = |L(x)+R(x)|^2 = &(Re[L(x)]+Re[L(x)])^2 \\ &(Im[L(x)]+Im[R(x)])^2 \end{aligned} \quad (4)$$

The two pairs of matched dyadic squares, belonging respectively to the right image $R(x)$ and the left image $L(x)$ must have the same orientation and the same size.
When we replace $L(x) = \rho_l(x)\exp(\phi_l(x))$and $R(x) = \rho_r(x)\exp(\phi_r(x))$ by their respective definition, we obtain the following equation :

$$E(x) = \rho_l^2(x) + \rho_r^2(x) + 2\rho_l(x)\rho_r(x)cos(\Delta\phi(x)) \quad (5)$$

$E(x)$ is the energy of the response obtained by the binocular complex cell. When the both pairs of dyadic squares have not a same position, the right monocular response $R(x)$ is a shifted version of the left monocular responses $L(x)$, i.e. $R(x) = L(x-d)$. Similarly, when the phase signal is not the same between the pairs of dyadic squares $\phi(x) = \phi(x-d)$. From this, we can express the inter-ocular phase difference using a Taylor series of $\phi_l(x-d)$(Eq. 13):

$$\Delta\phi_l(x,d) = \phi_l(x) - \phi_r(x) = \phi_l(x) - \phi_l(x-d) = d\phi'_{l/r} + O[d^2] \tag{6}$$

Combining equation 13 with equation 12 gives us a useful characterization of a binocular energy as described by equation 14. As the disparity is increased slightly above zero, the binocular energy response decreases as the cosine of disparity times instantaneous frequency, $cos(d\phi'_{l/r})$.

$$\Delta\phi_l(x,d) = \phi_l(x) - \phi_r(x) = \phi_l(x) - \phi_l(x-d) = d\phi'_{l/r} + O[d^2] \tag{7}$$

In [3], authors showed that if the simple cells have not the same orientation, the disparity between them is useless. Fleet [5] defined this relation in the following way:

$$R(x) = \exp(i\Delta\psi)L(x-d) = \rho_l(x-d)\exp(\phi_l(x-d) + \Delta\psi) \tag{8}$$

$\Delta\psi$ denotes a phase shift between the couple of simple cells. So, the binocular energy of the left and the right pairs of dyadic squares are then related. The phase difference has now the form:

$$\Delta\phi_l(x,d,\Delta\psi) = \phi_l(x) - \phi_r(x) - \Delta\psi = d\phi'_{l/r} - \Delta\psi \tag{9}$$

Finally, the binocular energy(Eq. 14), computed by the complex cell for the both pairs of dyadic squares, is equal to:

$$E(x,d,\Delta\psi) = \rho_l^2(x) + \rho_r^2(x) + 2\rho_l(x)\rho_r(x)cos(d\phi_l' - \Delta\psi) \tag{10}$$

If $E(x)$ is above the threshold (h) both dyadic squares are matched otherwise they are not matched.

4. REFINEMENT OF THE BINOCULAR ENERGY MODEL (RBEM)

To refine the result of matching obtained with the binocular energy model, we proposed a model based on the work of *Hayashi et al.* [6]. The authors proposed a stereo model that reconstructs *3D* structures not only from disparity information of inter-ocular paired regions in stereo images but also from unpaired regions. In our model, we use depth detection cells and unpaired dyadic square detection cells. These cells model some properties of the LGB. If the images are relatively different the system shows instability in regions where the binocular rivalry is reproduced (particularly in occulted regions). $E_x(x_l,x_r)$ is a function which proposes an initial matching for each pair (section. 3), such that $x_l = (x_l, y)$ is a pair of dyadic squares in the left retinal images (x_r=(pair of dyadic square in the right retinal images). After computing E_x, we define a disparity selective cell $b(x_l,x_r)$(Eq. 2), its value is a binary function equal to 1 when dyadic squares pairs are $E(x) > h$ and 0 when dyadic pairs are $E(x) <= h$ (See section 3). Opposite to $b(x_l,x_r)$, $M(x_{l/r})$ is equal to 1 when $E(x) <= h$ and 0 when $E(x) > h$.

When $b(x_l,x_r) = 1$ both pairs of dyadic squares are treated by the function $d(x_l,x_r)$. This function is a reassessment of the binocular energy of both dyadic squares pairs, taking into account a set of stereoscopic binocular constraint. If this energy decreases below a threshold (h) the two pairs of dyadic square are separated ($E(x) = 0$). The uniqueness constraint (U_u)(Eq. 16) converges to 0 if the binocular matching of the two dyadic squares are unique otherwise it converges to a negative value. The occlusion constraint (U_o)(Eq. 17) allows defining a coherent order of dyadic square pairs by their spatial position. The cohesiveness constraint (U_c)(Eq. 15), verify the coherence of the matching made. The function v is a reassessment of the monocular energy of a dyadic square pair, which takes three monocular constraints as its input. The occlusion constraint (Eq. 20) ($V_{lo/ro}$) checks if the dyadic square belongs to an occulted area of the two images. The cohesiveness constraint (Eq. 19) ($V_{lc/rc}$) checks the continuity between occulted pairs of dyadic squares. The inter-ocular inhibition constraint ($V_{li/ri}$) (Eq. 18) allows detecting the dyadic squares having instability in the model, particularly the pairs of dyadic squares which match $d(x_l,x_r,t)$ (Eq. 11) and in the same time they are considered in the model like unpaired dyadic squares.

$$d(x_l,x_r,t) = max(u(x_l,x_r,t)) \tag{11}$$

$$\frac{\partial u(x_l,x_r,t)}{\partial t} = -u(x_l,x_r,t) + b(x_l,x_r) + 2*U_u + 2*U_o + 10*U_c \tag{12}$$

U defines a set of pairs of dyadic squares of the right image for each pairs in the left image at instant t. This function takes as input parameters the result obtained at the instant $t-1$ and the result obtained by the function $b(x_l,x_r)$, by taking into account stereo constraints. $\phi(x_{l/r},t)$(Eq. 13) is the output of an unpaired dyadic square detection cell, representing whether a point at x_l in the left eye is interocularly unpaired or not at time t. v determine at a moment t if a coefficient is unpaired or not. This function takes as its input parameters the result obtained by the function $M(x_*)$(Eq. 3) and a set of monocular constraints.

$$\phi(x_{l/r},t) = max(v_{l/r}(x_{l/r},t)) \tag{13}$$

$$\frac{\partial v_{l/r}(x_{l/r},t)}{\partial t} = -v(x_{l/r},t) + m_{l/r} + 2*V_{lu/ru} + 2*V_{lo/ro} + 10*V_{lc/rc} \tag{14}$$

$$\begin{aligned} U_c = &\sum_{\xi_l<x_l \& \xi_r<x_r}^{left} \left[\begin{array}{l} w(\xi_l - x_l, \xi_r - x_r) * \\ (1 - P_r(\xi_r,x_r,t)) * \\ \left\{ \begin{array}{l} (1 - P_l(\xi_l,x_l,t)) \\ +\phi_l(x_l,t) * \\ (1 - G_l(\xi_l,x_l,t)) \end{array} \right\} * \\ d(\xi_l,\xi_r,t) \end{array} \right] \\ &+ \sum_{\xi_l>x_l \& \xi_r>x_r}^{right} \left[\begin{array}{l} w(\xi_l - x_l, \xi_r - x_r) * \\ (1 - P_l(\xi_l,x_l,t)) * \\ \left\{ \begin{array}{l} (1 - P_r(\xi_r,x_r,t)) \\ +\phi_r(x_r,t) * \\ (1 - G_r(\xi_r,x_r,t)) \end{array} \right\} * \\ d(\xi_l,\xi_r,t) \end{array} \right] \end{aligned} \tag{15}$$

$$\begin{aligned} U_u = &- \sum_{\xi_l>x_l}^{Near} (1 - \phi_l(x_l,t) + \phi_r(x_r,t))\, d(\xi_l,x_r,t) \\ &- \sum_{\xi_l>x_l}^{Far} (1 - \phi_l(\xi_l,t) + \phi_r(x_r,t))\, d(\xi_l,x_r,t) \\ &- \sum_{\xi_l>x_l}^{Near} (1 - \phi_r(x_r,t) + \phi_l(x_l,t))\, d(x_l,\xi_r,t) \\ &- \sum_{\xi_l>x_l}^{Far} (1 - \phi_r(\xi_r,t) + \phi_l(x_l,t))\, d(x_l,\xi_r,t) \end{aligned} \tag{16}$$

$$U_o = \sum_{\xi_l<x_l}^{Far} \phi_l(\xi_l,t)\,(1-N_r(\xi_l,x_r,t))\,d(\xi_l,x_r,t) + \sum_{\xi_r>x_r}^{Far} \phi_r(\xi_r,t)\,(1-N_l(x_r,\xi_r,t))\,d(x_r,\xi_r,t) + \phi_l(x_l,t)\,N_l(x_l,x_r,t) + \phi(x_r,t)\,N_r(x_l,x_r,t) \quad (17)$$

$$V_{li/ri} = -\sum_{x_r/x_l} \phi_{l/r}(x_{r/l},t)\,d(x_l,x_r,t) \quad (18)$$

$$V_{lc/rc} = \sum_{x_{r/l}} N_{r/l}(x_l,x_r,t)\,d(x_l,x_r,t) \quad (19)$$

$$V_{lo/ro} = \begin{cases} 1 \;\; if \;\; \exists \;\; \xi_{l/r} \;\; such \;\; that \;\; \phi_{l/r}(\xi_{l/r},t)=1 \\ 0 \;\; \text{otherwise} \end{cases} \quad (20)$$

$$w(\xi_l,x_l,\xi_r,x_r) = \exp\left(-\frac{1}{2\sigma_\Gamma^2}\Gamma^2\right)\exp\left(-\frac{1}{2\sigma_{x_c}^2}\Delta x_c^2\right) \quad (21)$$

w is a weighty function used in the coherence constraint. This function allows to check the variation of the disparity between the nearby coefficients. Γ (Eq. 22) represent the gradient of the disparity used by the function w. where $\Delta d = (\xi_l - x_l) - (\xi_r - x_r)$ and $\Delta x_c = \{(\xi_l - x_l) + (\xi_r - x_r)\}/_2$.

$$\Gamma = \left|\frac{\Delta d}{\Delta x_c}\right| \quad (22)$$

$\mu_{l/r}$ (Eq. 23 and Eq. 24)corresponds respectively to the boundaries of the unpaired coefficients in the right and the left images.

$$\mu_l(x_l,t) = \phi(x_l-1,t)\,(1-\phi(x_l,t)) \quad (23)$$

$$\mu_r(x_r,t) = \phi(x_r+1,t)\,(1-\phi(x_r,t)) \quad (24)$$

$P_{l/r}$ is a binary function, which takes the value 1 if there are unpaired coefficients, in the neighborhood of a given coefficient, otherwise it takes the value 0.

$$P_{l/r}(\xi_{l/r},x_{l/r},t) = \begin{cases} 1 \;\; if \;\; \phi_{l/r}(s_{l/r},t)=1 \;\; such \;\; that \;\; \xi_{l/r} \le s_{l/r} \le x_{l/r} \\ \text{otherwise} \end{cases} \quad (25)$$

$G_{l/r}$ is a binary function, which takes the value 1 if there are boundaries of unpaired coefficients in the neighborhood of a given coefficient, otherwise it takes the value 0.

$$G_{l/r}(\xi_{l/r},x_{l/r},t) = \begin{cases} 1 \;\; if \;\; \mu_{l/r}(s_{l/r},t)=1 \;\; such \;\; that \;\; \xi_{l/r} < s_{l/r} < x_{l/r} \\ \text{otherwise} \end{cases} \quad (26)$$

Contrary to $P_{l/r}$, $N_{l/r}$ is a binary function which takes the value 1 if it has not unpaired coefficients, in the neighborhood of a given coefficient, otherwise it puts itself in 0.

$$N_l(x_l,x_r,t) = \begin{cases} 1 \;\; if \;\; d(x_l,\xi_r,t)=1 \;\; such \;\; that \;\; \xi_r < x_r \\ 0 \;\; \text{otherwise} \end{cases} \quad (27)$$

$$N_r(x_l,x_r,t) = \begin{cases} 1 \;\; if \;\; d(\xi_l,x_r,t)=1 \;\; such \;\; that \;\; \xi_l > x_l \\ 0 \;\; \text{otherwise} \end{cases} \quad (28)$$

5. EXPERIMENTAL RESULTS

In this section, we present the results obtained with our stereoscopic matching model. Our model must be used with rectified stereoscopic images. Two pairs of rectified stereoscopic images are used to generate the obtained results (fig. 2.a). In the left image of the second pair, we added an object which does not exist in the right image, to see the behavior of our system in the case that the right and the left images have a major difference. Our model attributes to the dyadic square pairs (L(x) and R(x)) different colors according to their matching. So, we have defined four type of matching in our model. The similar regions, in both images matched are represented with the blue color. The occulted regions in both images are colored in black. These two colors appear in the solution computed by the BEM model (Section. 3). This solution is optimized by the refinement model (RBEM). This last one (Section. 4) models some properties of the LGB. The LGB classifies the information of both retinal images according to their spatial position. So, two informations belonging respectively to the left and the right images and which represent the same region of the space are put side by side. The association of three binocular constraints and the monocular constraints allow our model to converge on this property appropriate for the LGB.

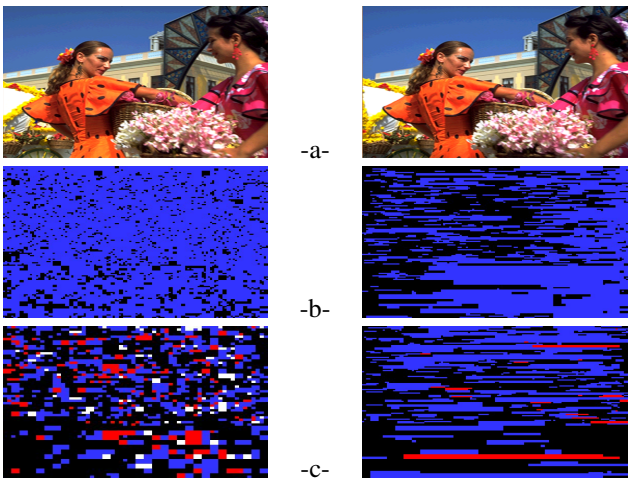

Fig. 2. Results obtained with our model using stereoscopic images (a) stereoscopic images (b) solution obtained with BEM (c) solution obtained with RBEM

Depth detection cells (Eq. 11) exploit the binocular constraint to increase the binocular energy of dyadic squares which respect these constraints and to converge the binocular energy of dyadic squares not respecting these constraints decreases. Unpaired dyadic square detection cells (Eq. 13) exploit the monocular constraints to increase the monocular energy of dyadic squares which respect these constraints and to converge the monocular energy of dyadic squares not respecting them decreases. Depth detection cells and unpaired dyadic square detection cells present an inverse correlation which varies according to the stereoscopic images used.

The blue squares represent dyadic squares belonging to

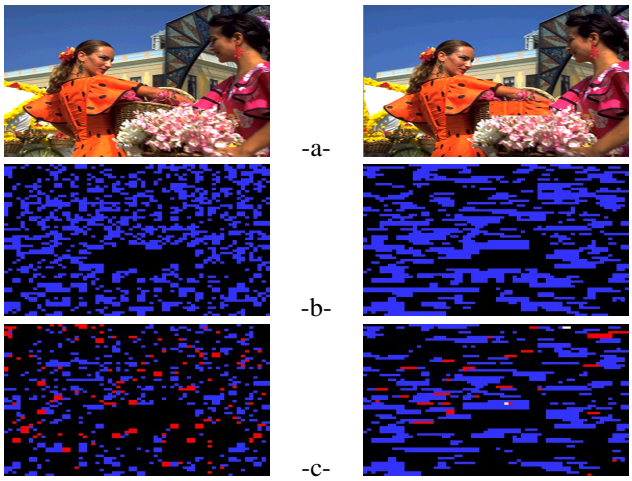

Fig. 3. Results obtained with our model using stereoscopic images with very different content (a) stereoscopic images (b) solution obtained with BEM (c) solution obtained with RBEM

the left and the right images having a strong binocular energy (Eq. 11)(fig. 2) and no monocular energy (Eq. 12). The red dyadic squares have a strong binocular energy and a strong monocular energy and they are matched with dyadic squares which have a strong binocular energy and no monocular energy. These dyadic squares belong to occulted regions in the left and right images. At the same time, this dyadic squares are similar to the dyadic squares of the redundant regions in both images. White dyadic squares have a strong binocular energy and a strong monocular energy and they are matched with dyadic squares which have a strong binocular energy and a strong monocular energy. These dyadic squares represent a case of instability in our model because both dyadic squares matched do not belong to both stereoscopic images and do not present any correlation with nearby dyadic squares.

Dyadic squares with the black color have an opposite behavior than white dyadic squares(fig. 3). The binocular energy and monocular energy of these black dyadic squares are low or equal to 0. Our model has several parameters which are fixed according to the stereoscopic images that we use, In the BEM model we have the parameter (h). If the binocular energy of a dyadic square couple is greater than the threshold(h) these last ones are matched. In the model of refinement we find that the parameter (h) also appears in the functions (Eq. 10, 11, 13). This parameter does not take the same value automatically in all the functions. To fix this threshold we compute the binocular energy for every pair of dyadic squares (Fig. 4.c). We compute the histogram (Fig. 4) of the obtained binocular energy map, according to that we define the compatible threshold for every function. The number of blue dyadic squares, red dyadic squares, white dyadic squares and black dyadic squares varies depending on the threshold (h).

6. CONCLUSION

In this paper, we proposed a model for stereoscopic matching, which can be exploited by 3D applications, as the 3D reconstruction, the stereoscopic coding, the stereoscopic quality assessment. To conceive this model we proceed in two steps. In the first step, we proposed a model of stereoscopic matching based on the human visual system (HVS) functions, particularly the simple cells and the complex cells functions, which merge the both retinal images in HVS. In the second step we proposed a model to refine the result obtained with the first model. This model uses some LGB properties. It takes as input a set of binocular stereoscopic constraints and monocular constraints to refine the matching computed in the first step. With this refined model, we obtain a more precise classification according to the type of regions, to which dyadic squares belong. The future directions of this work can be summarized by a psychophysical experiment allowing the validation of the proposed model.

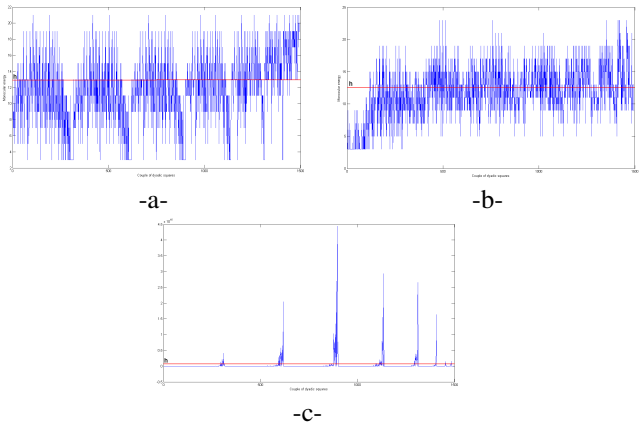

Fig. 4. Histogram of energy (a) left monocular energy (Eq. 14 for the left image). (b) Right monocular energy (Eq. 14 for the right image). (c) binocular energy (Eq. 12)

REFERENCES

[1] TN. Hubel, DH. Wiesel, "Stereoscopic vision in macaque monkey. cells sensitive to binocular depth in area 18 of the macaque monkey cortex," *Nature*, vol. 225, no. 41-42, 1970.

[2] GF. Enroth-Cugell C. Campbell, FW. Cooper, "The spatial selectivity of the visual cells of the cat," *J Physiol*, vol. 203, pp. 223–235, 1969.

[3] GC. Freeman-RD. Ohzawa, I. DeAngelis, "Stereoscopic depth discrimination in the visual cortex: neurons ideally suited as disparity detectors," *Science*, vol. 249, pp. 1037–1041, 1990.

[4] M.-C. Larabi, V. Brodbeck, and C. Fernandez-Maloigne, "A novel approach for constructing an achromatic contrast sensitivity function by matching.," in *IEEE International Conference on Image Processing (ICIP)*, Atlanta, GA, October 2006, pp. 441–444.

[5] D.J. Fleet, H. Wagner, and D.J. Heeger, "Neural encoding of binocular disparity: Energy model, position shifts and phase shifts," *Vision Research*, vol. 36, no. 12, pp. 1839–1857, 1996.

[6] R Hayashi, S Shimojo, and S Tachi, "An integrative model of binocular vision: a stereo model utilizing interocularly unpaired points produces both depth and binocular rivalry," *Vision Research*, vol. 44, no. 3, pp. 2367–2380, 2004.